Climate simulation of the 21st century with interactive land-use changes

Aurore Voldoire, Bas Eickhout, Michiel Schaeffer, Jean-François Royer, Fabrice Chauvin

Climate simulation of the 21st century with interactive land-use changes

Aurore Voldoire[(1)], Bas Eickhout[(2)], Michiel Schaeffer[(3)],

Jean-François Royer[(1)] , Fabrice Chauvin[(1)]

[(1)] Météo-France, Toulouse, France

[(2)] Netherlands Environmental Assessment Agency (MNP, formerly RIVM), Bilthoven, The Netherlands

[(3)] Wageningen University, The Netherlands

Corresponding author address:

A.Voldoire,

Météo-France,

CNRM/GMGEC/UDC,

42 avenue G. Coriolis,

31057 Toulouse Cedex 1

France

E-mail: aurore.voldoire@meteo.fr

Tel: (33) 5 61 07 96 98 – Fax: (33) 5 61 07 96 10

Abstract

To include land-use dynamics in a General Circulation Model (GCM), the physical system has to be linked to a system that represents socio-economy. This issue is addressed by coupling an integrated assessment model, IMAGE2.2, to an ocean-atmosphere GCM, CNRM-CM3. In the new system, IMAGE2.2 provides CNRM-CM3 with all the external forcings that are scenario dependent: greenhouse gas (GHGs) concentrations, sulfate aerosols charge and land cover. Conversely, the GCM gives IMAGE changes in mean temperature and precipitation.

With this new system, we have run an adapted scenario of the IPCC SRES scenario family. We have chosen a single scenario with maximum land-use changes (SRES A2), to illustrate some important feedback issues. Even in this two-way coupled model set-up, land use in this scenario is mainly driven by demographic and agricultural practices, which overpowers a potential influence of climate feedbacks on land-use patterns. This suggests that for scenarios in which socio-economically driven land-use change is very large, land-use changes can be incorporated in GCM simulations as a one-way driving force, without taking into account climate feedbacks. The dynamics of natural vegetation is more closely linked to climate but the time-scale of changes is of the order of a century. Thus, the coupling between natural vegetation and climate could generate important feedbacks but these effects are relevant mainly for multi-centennial simulations.

Introduction

There are two main factors that govern the distribution of vegetation over the continents: climate change and anthropogenic land use. In this study we will refer to the first factor as natural vegetation dynamics and to the second one as land-use dynamics, the two aspects will be involved in the term land cover change. Most of the time, the two aspects have been studied separately. The land-use issue was first studied through deforestation studies (Henderson-Sellers et al, 1993, Sud et al., 1996, Lean and Rowntree, 1997) which were quite simplistic. More realistic studies have been published in the last decade: they consist in comparing the climate simulated with an actual land cover map and with a natural land cover map where agricultural areas are replaced by natural vegetation. Among these studies, Zhao and Pitman (2002), Pitman and Zhao (2000), Chase et al. (2000) have shown that the impact of land-use change was relatively important, at least regionally. In particular, Bounoua at al. (2002) have obtained a warming in the tropics and a cooling in high latitudes that cancel each other when averaged globally, emphasizing the regional nature of land-use change studies. Govindasamy et al. (2001) and Bertrand et al. (2002) have also suggested that past climate changes could be partly attributed to land use changes. In their recent study, Matthews et al. (2004) have addressed the question of land-use in a transient experiment of the 20th century, but when land-use is externally forced, they could not detect the impact of land-use change on the global temperature. However, their study was limited to detection at the hemispheric scale which has already been shown not to be relevant. Additionally, DeFries et al. (2002); Feddema (2005b) and Voldoire (2006) have addressed the issue of future land-use changes and concluded that future land-use change could amplify or modulate the resulting climate change, depending on location.

The issue of natural vegetation dynamics was first investigated with equilibrium vegetation models, mainly BIOME (Prentice et al., 1992) which evaluates the vegetation distribution that is in equilibrium with a given climate. Braconnot et al. (1999) showed that

accounting for vegetation changes in the mid-Holocene improved simulation of the African monsoon. Dynamical global (natural) vegetation models (DGVM) for coupling to General Circulation Models (GCMs) have recently been developed (Foley et al. 1996; Sitch et al. 2003). These models simulate carbon fluxes at the time-step of the model and predict transient changes in vegetation structure based on the carbon balance and competition among plants. With such models, Notaro et al. (2005) have shown that the greening in high latitudes could be attributed to rising levels of carbon dioxide. Delire et al. (2004) have shown that coupling a DGVM to a GCM alter the long term variability of precipitation over land. Concerning the African monsoon, Wang et al. (2004) have found that natural vegetation dynamics can only partially sustain the Sahel drought and suggested that the land-use changes that are missing in such models may have also contributed to the Sahel drought (as shown by Taylor et al., 2002). This study points out the need to include both natural land cover change and land-use changes in study of the 20th century and of the future. However, there are only a few studies that have addressed both effects. Matthews et al. (2004) have included both in a simulation of the 20th century, and they found that vegetation induced a positive feedback effect on the simulated climate change. However, in their study only natural vegetation was dynamically simulated, while land-use was externally forced.

For simulations of the 21st century climate, the question of land-use should be as important as over the 20th century since the anthropogenic pressure is expected to increase. Similarly, climate change (and rising levels in carbon dioxide) could alter the natural vegetation distribution. Figure 1 represents the change in Leaf Area Index (LAI) resulting from vegetation change as simulated by the Integrated Model to Assess the Global Environment (IMAGE; Alcamo et al., 1998) model between 2090-2099 and 1970-1979 for the A2 scenario of the Intergovernmental Panel on Climate Change (IPCC). As further explained in section 2.1, IMAGE calculates a natural vegetation map accounting for climate change and CO_2 effects, and an anthropogenically influenced land cover map where land use is accounted for. The natural vegetation map corresponds roughly to what can be simulated with more complex

DGVMs. When only natural vegetation is considered, the LAI is expected to increase in the tropics, mainly due to the increase in fertility caused by the increase in atmospheric CO_2. However, when land use is also accounted for, LAI decreases in the tropics as a consequence of deforestation in this particular A2 scenario. This highlights the absolute need to take into account land-use change when attempting to make realistic projections over the 21st century with a DGVM. Note that there are some studies with DGVMs which simulate a negative impact on natural vegetation in some regions, contrary to what is simulated here by IMAGE. Feddema et al. (2005b) have run a 21st simulation in which land cover is modified according to IMAGE projections, and have shown that it has a significant impact on regional and seasonal simulated climate change. However, in their study, the change in land cover is imposed and thus neglects possible feedbacks between climate and vegetation.

It can be concluded that this feedback needs to be investigated. This requires the inclusion of a socio-economic model in physically based GCMs. The issue of introducing economic considerations in a physical system has already been addressed within integrated assessment models (IAMs). These models have been designed to represent consistently, but in a highly simplified way, the different aspects of the earth system involved in the climate change issue, from economics to physics. A first generation of these models, called evaluation models, have been widely used to produce emission scenarios of GHGs for IPCC's Third Assessment Report (Houghton et al. 2001): taking different demographic and economic scenarios, the IAMs have evaluated the energy consumption, the food requirements and the resulting emissions. Amongst these models, IMAGE2.2 (Alcamo et al. 1998) has the added value of simulating the evolution of land cover on a spatial grid. This aspect is important for IAMs since vegetation plays a crucial role in representing terrestrial carbon reservoirs. The disadvantage of integrating multi-disciplinary aspects of the climate system is that IAMs are based on simpler formulations than state-of-the-art models within each discipline. As a first step toward a consistent evolution of natural land cover and land-use in GCM experiments, we propose here an original method: coupling a GCM to the IMAGE2.2 IAM in order to

simulate dynamically the land cover, including land-use changes, in scenario simulations. Even if the land cover simulation can be considered as somewhat crude compared to more elaborated models, the method proposed here has the advantage of simple implementation, while the computer-time cost of running the GCM is only marginally increased by the IMAGE-2.2 IAM. Such a coupling will provide an idea of the relevance of including the land-use dynamics in a GCM and could help designing future models of land-use to be coupled with GCMs.

1. Initial Models

1.1. The IMAGE2.2 model

Overview

IMAGE 2.2 is a dynamic integrated assessment modeling framework for global change (Alcamo et al. 1998 and http://www.mnp.nl/image/). The main objectives of IMAGE are to contribute to scientific understanding and support decision-making by quantifying the relative importance of major processes and interactions in the society-biosphere-climate system. In the IMAGE2.2 framework, the general equilibrium economy model, WorldScan, and the population model, PHOENIX, feed the basic information on economic and demographic developments for 17 world regions into three linked subsystems (figure 2):

- The Energy-Industry System (EIS), which calculates regional energy consumption, energy efficiency improvements, fuel substitution, supply and trade of fossil fuels and renewable energy technologies. On the basis of energy use and industrial production, EIS computes emissions of greenhouse gases (GHG), ozone precursors and acidifying compounds.

- The Terrestrial Environment System (TES), which computes land-use changes, on a 0.5° resolution grid, on the basis of regional consumption, production and trading of food, animal feed, fodder, grass and timber, with consideration of local climatic and terrain

properties. TES computes emissions from land-use changes, natural ecosystems and agricultural production systems, and the exchange of CO_2 between terrestrial ecosystems and the atmosphere.

- The Atmospheric Ocean System (AOS) calculates changes in atmospheric composition using the emissions and other factors in the EIS and TES, and by taking oceanic CO_2 uptake and atmospheric chemistry into consideration. Subsequently, AOS computes changes in climatic properties by resolving the changes in radiative forcing caused by greenhouse gases, aerosols and oceanic heat transport.

Land cover dynamics

The IMAGE2.2 land cover model evaluates land cover following three steps.

(1) Estimation of the **Potential land cover**: this is the distribution of natural vegetation that is in equilibrium with a given climate. This map is evaluated with the BIOME model (Prentice et al. 1992) adapted to the land cover classes used in IMAGE2.2 (Leemans and van den Born 1994). The BIOME model takes into account the mean climate, in terms of monthly temperature and soil moisture availability, to compute the dominant vegetation type in a given grid box. This version of BIOME also considers the increase in water use efficiency due to an increase in atmospheric CO_2 concentration. The main drawback of the potential vegetation approach is that the assumption of equilibrium of vegetation with climate is not valid for climate change studies where the time-scale of climate change is much shorter that the adaptation time-scale of vegetation. One of the main strengths of the IMAGE2.2 model is to propose a method to limit vegetation changes according to transition rules (Van Minnen et al., 2000).

(2) The **natural land cover** is an adaptation of the potential vegetation given transition time and seed dispersion limits. Given the natural vegetation map of the last time step, for each grid point where the new potential vegetation is different to the former natural vegetation, the possibility of transition is decided according to the distance from where the potential new plant functional type (PFT) is already present. The seed dispersion limit is itself

dependent on the PFT. The model also takes into account that the transition cannot be immediate. The length of the transition phase depends on the PFT (one or 2 decades for low vegetation types and up to 80 years for tree species). At this stage, no anthropogenic interference with the land cover is present.

(3) The third step consists in including land-use change in the land cover to obtain an **actual land cover** map. As a prerequisite, IMAGE has calculated the need in wood, grasslands and crops for the 17 regions considered; and has calculated a productivity of each grid cell for each type of use. The productivity evaluation of crops is based on the Agro-Ecological Zones project (Fisher et al. 2000) from the Food and Agriculture Organization (FAO). Then, the issue is to choose where to cultivate, where to afforest, where to breed. The distribution of agricultural land in 1970 is based on FAO statistics for the size of agricultural area per country and satellite data for location preferences. Afterwards, if food demand is not met, new arable land grid points are set depending on the following criteria: crop productivity (the higher the productivity, the higher the preference to expand arable land there), distance to other croplands, distance to regions of high population density and distance to water reservoirs. The same is done for pasture land and wood production (although crop productivity is not one of the criteria for wood). To account for non-rule behavior of people, the deterministic choices in the model are slightly modified by adding a random factor in the preference dedication. At the end of the simulation year, when all the demands are met, the remaining grid points keep their natural vegetation. On figure 1, the case called "Natural vegetation only" corresponds to the change in LAI given by the natural land cover map everywhere (step 1 and 2). The case called "Natural vegetation + land-use" is the result of the actual land cover map calculation (all steps included).

1.2. The CNRM-CM3 GCM

We use the CNRM coupled general circulation model CNRM-CM3 (Salas-Mélia et al., 2006). This model has been used to run simulations for IPCC's Fourth Assessment Report and is composed of the ARPEGE atmospheric model (Déqué et al., 1999), the OPA8.1

oceanic model (Madec et al. 1997), the GELATO sea-ice model (Salas-Mélia, 2002), the land surface scheme ISBA (Mahfouf et al. 1995), the TRIP river routing scheme (Oki and Sud 1998) and the MOBIDIC ozone chemistry model (Cariolle and Déqué 1986). All these models are linked through the OASIS coupler (Terray et al. 1998) developed at CERFACS. This version of the GCM is documented in Salas-Mélia et al. (2006), and will only be described briefly here.

ARPEGE is a spectral model with a progressive hybrid sigma-pressure coordinate and a two-time-level semi-Lagrangian semi-implicit integration scheme (Côté and Staniforth 1988). For this study, we have used a T63 triangular truncation, with 45 levels in the vertical up to 0.05hPa. Physical parameterizations include the turbulence scheme of Louis et al. (1982), the statistical cloud scheme of Ricard and Royer (1993), and the radiative scheme of Morcrette (1990), which includes the effect of several greenhouse gases (CO_2, CH_4, N_2O and CFCs), water vapor, ozone as well as the direct effect of four aerosols types (marine, desert dust, black carbon and sulfates). For convection, the Bougeault (1985) mass-flux convective scheme with Kuo-type closure is used. The ISBA land surface scheme simulates the exchange of energy, water and momentum at the land-atmosphere interface. Note that the version employed here does not simulate carbon fluxes.

The OPA8.1 ocean model, developed at LODYC (France), is a finite difference model (Madec et al. 1997). It is based on primitive equations in which the thin shell, hydrostatic and Boussinesq approximations are assumed. The rigid lid assumption is made, so that surface gravity waves are filtered. The ocean model is spatially discretized on a three-dimensional generalization of the Arakawa C-grid. The horizontal resolution is approximately 2° in longitude and, in latitude, varies from 0.5°at the equator to 2° in polar regions. The time-step for coupling ocean and atmosphere is 1 day.

2. The coupling system CNRM-CM3/IMAGE2.2

2.1. The coupling method

In its standard version, the IMAGE 2.2 climate module is based on the MAGICC model (Hulme et al. 2000), and is composed of a simple radiative balance scheme for the atmosphere and a diffusion-upwelling oceanic model. This module calculates the change in global mean temperature associated to a given increase in GHGs concentrations. This global mean change is regionalized through the SCENGEN model technique (Hulme et al. 2000), which consists in projecting the global change on a fixed pattern of climate change due to an increase in GHGs concentration. To account for non-linear responses of sulphur aerosols, the downscaling method is elaborated with additional profiles for sulfate aerosols (Schlesinger et al., 2000). The implementation of these models in IMAGE2.2 is detailed in Eickhout et al. (2001). To couple CNRM-CM3 with IMAGE, we have simply replaced the climate module with the GCM, i.e. IMAGE provides GHGs, aerosols and land cover map to the GCM which in turn simulates the corresponding climate change and this change is given back to the IMAGE2.2 model as pictured in figure 3. In IMAGE, the climate change is only represented by the change in temperature and precipitation (other climate parameters such as cloud cover are kept constant). This climate change is fed back to the terrestrial environment system, and to the oceanic carbon model in IMAGE2.2. The oceanic carbon model is based on the Bern CC model (Joos et al., 1996). It takes the ocean temperature as an external forcing and calculates the carbon flux to the ocean using an iterative method to maintain an equilibrium between the atmospheric and oceanic CO_2 concentration.

In the new system, the carbon cycle is determined in IMAGE whereas temperature and precipitation evolution are determined by CNRM-CM3 and there is no discrepancy in the coupling. The only aspect that could be improved in a future version of the coupling concerns the water balance that is re-estimated in IMAGE based on monthly precipitation.

The coupling time-step between IMAGE and CNRM-CM3 is 5 years, which is also the time-step of the land cover model in IMAGE. As is explained in section 2.1, the natural land cover is produced by using the BIOME model that operates with a mean climate, and is not designed to account for climate variability. This is also the case for the AEZ crop productivity model. For this reason, it has been decided to give IMAGE a mean change in climate calculated over the last current 30 years of the climate simulation. This means that, for instance in 2050, the GCM provides IMAGE with a change in mean climate calculated as the difference between the average over the period 2020-2049 compared to the reference period 1960-1989. One of the major drawbacks of this method is the time-lag introduced, since the mean climate change corresponds more to a change between 2035 and 1975 than to a change between 2050 and 1990. However, the need to use a mean climate change requires the use of such an approach.

In the new coupled system, in addition to the land cover maps, IMAGE provides CNRM-CM3 with all the forcings that are scenario-dependent and that were usually prescribed exogenously in CNRM-CM3. This includes the GHGs concentrations (CO_2, CH_4, N_2O, CFCs), the sulfate aerosols concentrations and the concentration in chemical species relevant to the ozone chemistry. IMAGE has participated in the definition of the emission scenarios provided in the IPCC report (Nakicenovic et al. 2001) that are currently used to run scenario simulations. This means that given a scenario path (A2, B2, B1, A1), IMAGE is one of the models that can produce the corresponding emission scenario. All the IAMs that have participated in the IPCC report have run all the scenarios, but each model has provided the "marker" for one scenario. In this framework, IMAGE2.2 has supplied the IPCC B1 emission scenario. This means that emission scenarios provided by IMAGE are quite consistent with those given in the IPCC report; however, there can be marginal differences.

2.2. Simulation performed

One simulation with the new coupled system has been performed. We have chosen to run an A2 scenario, because changes in land cover (and particularly in land use) are the most

widespread for this scenario. Deforestation persists until the end of the 21st century given the constant increase in population combined with high food demands and little trade between regions. Other SRES scenarios show less deforestation and even reforestation after 2050 in A1 and B1. Moreover, the results can be compared with an earlier A2 simulation using the "stand-alone" CNRM-CM3 model. IMAGE is designed to begin simulations in 1970 and is run using observed climate until 1995. The effective start date of the coupled scenario simulation is thus 1995. However, CNRM-CM3 is started in 1940, and is initialized with the climate state given in 1940 by a former IPCC simulation of the 20th century run with CNRM-CM3 (called 20C3M in Salas-Mélia et al. 2006). The model is then run for 30 years with constant forcings given by IMAGE for year 1970. Then, forcings including land cover evolve according to the IMAGE projections, but there is no feedback to IMAGE before 1995. The coupled system is then run from 1995 to 2100 and the simulation is called A2-IM-CM3.

In the following, this simulation is compared to a former A2 scenario simulation with the same CNRM-CM3 model, called A2-CM3. In this simulation, the land cover is fixed to the actual land cover map. As discussed in section 2.1, it must be stressed that A2-CM3 has been run using forcings given by IPCC that are slightly different from those produced commonly by the IMAGE model, since the IPCC forcings were produced by another IAM (figure 4). This means that the difference in forcings used in A2-IM-CM3 and in A2-CM3 is explained not only by the coupling, but also by the fact that they comes from two different IAMs.

To analyze the impact of the coupling on the emission scenario itself, we compare the forcings produced in the A2-IM-CM3 simulation to those produced by IMAGE in its standard configuration, i.e. with its simpler climate module. This simulation is called A2-IM. We also performed an IMAGE simulation in which the climate change produced by the GCM alone (A2-CM3) is used to drive the IMAGE model (no use of its simple climate module and no feedback of IMAGE on the GCM simulation). This simulation is called A2-IM-forced.

3. Results

Before presenting the results, several remarks have to be made. First, running a single experiment does not allow us to analyze in detail the impact of using a dynamical coupling between vegetation and land-use. It has already been shown that the climate impact of land-use change is of second order as compared to the impact of increasing the GHGs concentrations (Voldoire 2006, Pitman and Zhao 2000), at least at the global scale. A thorough analysis would require an ensemble of control experiments and an ensemble of experiments with the new system CNRM-CM3/IMAGE2.2. There are even several ways to build these experiments. The best would be to run 3 different simulations: one with fixed vegetation, one with vegetation changes forced (no interaction) and one with the interaction between vegetation and climate. The simulation described here has to be seen as a first attempt to couple a GCM with models based on economical considerations. This study leads to several conclusions which should be interpreted as recommendations for future developments.

3.1. Greenhouse gas concentration scenario

The GHGs concentration scenario is quasi-identical in all IMAGE simulations (figure 4), whether or not the climate change is prescribed or simulated with a simple or a complex model. We know that concentrations in GHGs depend on climate in IMAGE (through emission from vegetation and from land-use changes, mainly deforestation), however, for all IMAGE simulations we obtain very similar concentration scenarios. This indicates that the coupling with the GCM has not significantly modified GHGs emissions, suggesting that emissions from industries largely dominates in an A2 scenario.

We can notice that there are only small differences between the forcings obtained with IMAGE and those given by the IPCC SRES that were used in A2-CM3. The noticeable difference is the larger concentrations of CH_4 obtained with IMAGE. As all IMAGE2.2 simulations produce the same methane scenario, it is clear that the difference comes from the

different interpretation of the A2 storyline that are made in IMAGE and in the IAM that has been used to produce the SRES A2 scenario.

Global mean evolution

The annual mean global temperature simulated by the new coupled system (A2-IM-CM3) is rather similar to the CNRM-CM3 simulation until 2000 (A2-CM3). After 2000, there is a rather abrupt warming of about 0.5K that is not seen in the A2-CM3 simulation. The difference in mean temperature seems to persist throughout the 21st century (figure 5). The warming is associated to a sudden sea-ice melting as pictured in figure 6. Such an abrupt sea-ice melting is also observed in the A2-CM3 simulation, but later in the century (Figure 6b). To assess the significance of such a trend in sea-ice melting, we have calculated the same diagnostic in a simulation using constant pre-industrial forcings with CNRM-CM3. This simulation is 500 year long and thus resolves the natural variability of the CNRM-CM3 model. The trend simulated at the beginning of the 21st century in A2-IM-CM3 is out of the range of trends corresponding to the natural variability of the model, and is therefore attributable to a change in forcings.

At each grid point, we have calculated the first year in which the simulation A2-IM-CM3 becomes warmer than simulation A2-CM3 for ten years in a row in annual means (Figure 7). There are two regions where A2-IM-CM3 is warmer than A2-CM3 since 1970: Siberia and southeastern Africa. The warming over Africa has a limited geographical extent. On the other hand, the warming over Siberia is followed by a warming over the Artic ocean. This spread of the warming could explain the sea-ice melting that occurs at the beginning of the 21th century. Then, the question is why simulation A2-IM-CM3 is persistently warmer than A2-CM3 over Siberia?

This is due to a lower albedo over this region when using the IMAGE land cover distribution (annual mean albedo 0.25 in the A2-IM-CM3 simulation, instead of 0.35 in A2-CM3 - figure 8). In 1970, IMAGE covers much of the Siberian region with boreal forest (figure 12) that has a low albedo, whereas the ECOCLIMAP database (Masson et al. 2003)

used for the A2-CM3 simulation shows mostly tundra over this region. As the ECOCLIMAP database is derived from satellite products, it is not possible to plot a similar map as figure 12a for the A2-CM3 land cover map. To provide an idea of the difference between the A2-CM3 land cover map and A2-IM-CM3 land cover map in 1970, we have plotted the corresponding annual mean leaf area index for these two experiments on figure 9. The most noticeable difference is a more intense vegetation cover over boreal regions in A2-IM-CM3. Additionally, we observe a larger leaf area index on the border of deserts. This difference in land cover results in a very different vegetation albedo over boreal regions, which is further enhanced during the winter months due to the masking effect of forests on snow. This discrepancy of the IMAGE land cover has already been pointed out by Feddema et al. (2005a).

Therefore, the sea-ice melting is a consequence of the use of this different land cover database. The A2-IM-CM3 simulation uses this database starting from 1940 and we thought that 30 years (1940-1970) were enough as spin-up. It appears that a longer spin-up was necessary (probably more than 60 years) to reach an equilibrium.

Regional change

As mentioned in Bounoua et al. (2002) and in Voldoire (2006), land-use change has mainly an impact on the regional scale. From our experiment, we could expect that some regions have a stronger warming and others a weaker warming in simulation A2-IM-CM3 compared to simulation A2-CM3. Since the two simulations have a different global mean temperature responses, a direct comparison of the geographical anomalies of temperature change between the end of the 20^{th} century and the end of the 21^{st} century would mainly show the different level of warming in the two experiments, and this would mask the differences in their geographical patterns. To emphasize the impact of land cover change on the pattern of warming, we have displayed the annual mean change in near surface temperature normalized by the global mean change (figure 10). From this figure, it is hard to discriminate any impact of land cover change on the tropics. Over Africa for instance, the pattern is not very different

(stronger warming over the Sahara and southern regions of Africa). Note that in IMAGE2.2, the increase in crop area over Africa peaks in 2080 for an A2 scenario, thus over Africa it would be more appropriate to look at the climate change at this time. On the contrary, there is a significant warming over northern Europe. Over this region, crop area increases by 16% at the expense of forest area. In a former study with the same atmospheric model (Voldoire, 2006), it has been shown that the substitution of crops by forest leads to an increase in annual mean temperature over this region. We could thus expect that an increase in crop cover would reduce the temperature, contrary to what happens here. This suggests that the warmer temperature is not a consequence of a local land cover change. As A2-IM-CM3 is warmer over a large domain covering the Artic ocean, this differences could be attributed to the different evolution in sea-ice cover. However this can not be demonstrated with the experiments available at this time, it could also be attributed to a difference in sulfate aerosols forcing.

Concerning the impact on precipitation, it is also hard to find out significant differences in the pattern of change (figure 11). The most significant change appears over northern Amazonia. In the simulation A2-CM3 over South America, there is only a small region to the north of Amazonia where there is a decrease in precipitation. In the coupled simulation, this decrease extends southwards. This corresponds to the region where the change in land cover is the more intense in the IMAGE2.2 A2 scenario. Over this region, the model simulates a quasi-total deforestation (increase of crop area from 10% to 80% of the domain). Voldoire and Royer (2004) have already assessed the impact of such deforestation in the CNRM-CM3 model and have shown that it reduced the precipitation over northern Amazonia. It is also shown that in this model, the impact of deforestation on mean near surface temperature is not very large since there is a decrease in minimum temperature due to a stronger night-time cooling and a warmer maximum temperature. As a result, deforestation leads to an increase in the daily temperature range (DTR) at least during the dry season in the model. In figure 13, it can be seen that only the simulation with the land cover change (A2-IM-CM3) produces an

increase in DTR on average from July to November over the Amazonian region. This increase in DTR occurs together along with a decrease in evaporation, whereas all other climate simulations of the 21st century run with CNRM-CM3 produce an increase in evaporation over this region (not shown).

Voldoire and Royer (2004) have also shown that Amazonian land-use changes had a much larger impact on climate extremes. Here, we have calculated extremes indices over Amazonia as described in Frich et al. (2002) based on daily rainfall, minimum and maximum temperatures (table 2). For temperature, the change in indices is not very different between the coupled simulation and the non-coupled. We can only remark that changes in minimum temperature are reduced in the coupled simulation and the situation is reversed for the maximum temperature. On the contrary, for precipitation, indices reflect a quite different evolution over the 21st century. In the non-coupled simulation, the number of days with heavy rainfall increases significantly throughout the century whereas it is not changed significantly in the coupled simulation. Consistently, the maximum precipitation total over 5 consecutive days is decreased. The number of consecutive dry days does not change in the non-coupled simulation whereas it significantly increases in the coupled simulation. These changes in extremes are consistent with the former study by Voldoire and Royer (2004) and give some piece of evidence that the change in land cover has had an impact on the simulated climate change.

3.2. Is there any apparent feedback in the new system from the IMAGE2.2 point of view?

As mentioned earlier, it is not possible to analyze in detail the impact of the use of a dynamical land cover in CNRM-CM3 with only one simulation. However, if running the CNRM-CM3 model is computationally expensive, it is not the case of the IMAGE2.2 model. For this reason, we have investigated the question of feedbacks from the IMAGE point of

view. If strong feedbacks had happened in the coupled system, we could expect to find differences between a run with IMAGE alone and with IMAGE coupled to CNRM-CM3.

The case of northern Amazonia

Because we have found some indication that land cover change over northern Amazonia impacts the simulated climate, we could also expect that the land cover change is in turn affected by the change in climate. Cox et al. (2000) have shown that the feedback between climate and land cover plays a major role in Amazonia. To provide an idea of the variability of the IMAGE projections as well as to assess the impact of including a coupling with the CNRM-CM3 model, a set of IMAGE2.2 simulations has been run. It is composed of simulations for 3 different economic scenarios (A2, B1, A1B) and for each scenario, different changes in temperature and precipitation are imposed. These simulations are run with the IMAGE model without its climate module and not interactively coupled to CNRM-CM3. In this case, the change in temperature and precipitation are taken from existing GCM simulations performed with the CNRM-CM3 model and can be regarded as external forcings to the IMAGE model. We also used the climate change simulated in the new simulation A2-IM-CM3. The three IMAGE scenarios have also been run with that no changes in temperature and precipitation during in the 21st century (only a change in carbon cycle and anthropogenic pressure). The simulations are named SS_PTx where SS is the name of the SRES scenario chosen to run the IMAGE model and PTx refers to the change in temperature and precipitation used to run IMAGE. Simulations named SS_fix used constant precipitation and temperatures. In using different climate change simulations to run the same economic scenario, it is intended that the impact of the climate change used in the IMAGE simulation is estimated compared to the impact of the economic scenario chosen. The same color is used in the figures for simulations using the same economic narrative in IMAGE and the different line-styles refer to the different climate forcing used in IMAGE.

From figure 14a, it is obvious that the area of crops over Northern Amazonia is mainly driven by the economic scenario choice rather than by climate change. It is also clear that the

simulation with the new coupled system provides very similar results to the other A2 simulations. This emphasizes that future projections of agricultural land are mainly dependent on demographic and farming practices. The same conclusion can be drawn over all regions where the area of crops changes drastically. Such a result seems to be supported by Seguin (2005) who claims that farming activities can adapt to climate quite rapidly. However, in a less economically driven scenario, climate could play a more important role in land use dynamics, and feedbacks could become more important. This could be assessed by simulating other SRES scenarios with the IMAGE2.2/CNRM-CM3 coupled model.

It should be noted that our study suffers from several limitations. The major shortcoming of the coupled system used, is that land cover accounts only for mean climate change in temperature and precipitation. However, as seen in section 3.1, land cover change has an impact not only on mean climate but also on extremes. Conversely, it has been shown that a change in climate extremes could have a more severe impact on vegetation than a change in mean climate (Parmesan et al., 2000, Botta and Foley, 2002). Therefore, results could be somewhat different if climate variability was accounted for. However, this effect would be more crucial for scenario with more modest driving forces compared to the scenario evaluated in this paper. Another caveat concerns the sensitivity of the GCM to land cover change. As suggested in Voldoire and Royer (2004), the CNRM-CM3 model may have a quite weak sensitivity to land use changes compared to other GCMs. However, no comparison is actually possible since, even for tropical deforestation experiments, the experimental setups between models are quite different. Consequently, our experiment should be repeated with different GCMs to validate the results.

Natural vegetation

In IMAGE, the dynamics of land cover in the tropics is mainly driven by the need for agricultural land. Vegetation is less affected by human management in high latitudes. Over high latitudes, the increase in temperature is expected to produce a northward shift of the boreal tree line and of the tundra. Contrary to the case of Amazonia, figure 14b shows that the

change in land cover over high latitudes is mainly driven by climate. We could expect some feedback to happen there, however, with this experiment alone it is hard to detect an impact on the simulated climate. Moreover, the development of forest takes more than 50 years in IMAGE, consequently most of the changes seen on figure 12 are only just starting by the end of the simulation and we could expect a more important impact on climate in a longer term simulation. Feedback processes would probably become more important in longer term simulations.

4. Conclusions

A new system coupling a GCM, CNRM-CM3, and an integrated assessment model, IMAGE2.2, has been constructed. This new system allows the forcings traditionally used to run climate simulations of the future to be dynamically calculated in the IMAGE2.2 model according to the simulated climate change. With this new system, the GCM can use not only the evolving GHGs concentrations and aerosols, but also the changing land cover. Compared to more physically based dynamical models for vegetation, the approach used in IMAGE2.2 is much simpler, but it has the main advantage of including the land-use dynamics. Several research groups have developed dynamical vegetation models that they couple with GCMs, however, state-of-the-art dynamical vegetation models still do not include the land-use dynamics.

Only one simulation could be run with the new coupled system. Even if some problems exist, this first attempt provides some relevant information:

- Feddema et al. (2005a) have shown that the differences between different land cover map databases could be as large as realistic changes introduced in future land cover. For this reason, when using a new land cover database, it is necessary to run the model for several years to reach equilibrium. While the spin-up necessary in an atmospheric model alone is quite short, it is obvious from our experiment that this is not the case when using a coupled ocean-atmosphere model, due to sea-ice and ocean

retroactions. In coupled mode, it appears that more than 60 years may be necessary to reach equilibrium.

- We have chosen a scenario with maximum socio-economically driven land-use changes. In this scenario, the dynamics of land use is mainly driven by economy, demography and farming practices, and climate has only a second order impact on its evolution. Thus, for research groups who have developed a dynamical vegetation model coupled to a GCM, this suggests a quite simple implementation of land-use changes. As land cover changes are only marginally dependent on the simulated climate change, the regional evolution of agricultural areas could be taken as an external forcing factor, as done for GHGs concentrations or aerosols. In this way, they would avoid the problem of the lack of realism of ignoring future land-use changes (figure 1). However, this approach may not be valid in a less economically driven scenario where climate could play a more important role in land use dynamics, and feedbacks could become more important.

- The dynamics of natural vegetation is much more dependent on climate. However, in this study, we do not account for the change in climate variability (heat waves, extremes, etc) that could have a stronger impact on vegetation than mean climate change. Secondly, the time-scale of natural vegetation dynamics is on the order of several decades (especially for forest biomes) as is the time-scale of the response of the climate system. For this reason, feedbacks between climate and natural vegetation would probably appear in longer term simulations. The issue of natural vegetation dynamics is thus probably much more crucial for simulations over several centuries.

Acknowledgments

We wish to thank the anonymous reviewers whose comments and suggestions have greatly improved the paper. This work has been supported by the European

Commission Sixth Framework Program (ENSEMBLES contract GOCE-CT-2003-505539) .

References

Alcamo, J., R. Leemans and E. Kreileman (1998). Global modelling of environmental change: an overview of IMAGE 2.1. *Global change scenarios of the 21st century*. Elsevier Science. 3–96.

Bertrand, C., M. Loutre and M. Crucifix (2002). Climate of the last millennium: a sensitivity study. *Tellus*, *54A*, 221–244.

Botta, A. and J. Foley (2002). Effects of climate variability and disturbances on the Amazonian terrestrial ecosystems dynamics. *Global Biogeochem. Cycles, 16*. DOI: 10.1029/2000GB001338.

Bougeault, P. (1985). A simple parameterization of the large-scale effects of cumulus convection. *Mon. Weather. Rev.*, *113*, 2108–2121.

Bounoua, L., R. DeFries, G. Collatz, P. Sellers and H. Khan (2002). Effects of land cover conversion on surface climate. *Clim. Change*, *52*, 29–64.

Braconnot, P., S. Joussaume, O. Marti and P. de Noblet (1999). Synergistic feedbacks from ocean and vegetation on the African Monsoon response to mid-Holocene insolation. *Geophys. Res. Lett.*, *26*, 2481–2484.

Cariolle, D. and M. Déqué (1986). Southern hemisphere medium-scale waves and total ozone disturbances in a spectral general circulation model. *J. Geophys. Res.*, *91*, 10825–10846.

Chase, T., R. Pielke, T. Kittel, R. Nemani and S. Running (2000). Simulated impacts of historical land cover changes on global climate in northern winter. *Climate Dyn.*, *16*, 93–105.

Cox, P., R. Betts, C. Jones, S. Spall and I. Totterdell (2000). Acceleration of Global warming due to carbon cycle feedbacks in a coupled climate model. *Nature*, *408*, 184–187.

Côté, J. and A. Staniforth (1988). A two-time-level semi-Lagrangian semi-implicit scheme for spectral models. *Mon. Weather. Rev.*, *116*, 2003–2012.

DeFries, R., L. Bounoua and G. Collatz (2002). Human modification of the landscape and surface climate in the next fifty years. *Global Change Biology*, *8*, 438–458.

Delire, C., J. Foley and S. Thompson (2004). Long-term variability in a coupled atmosphere-biosphere model. *J. Climate.*, *17*, 3947–3959.

Déqué, M. (1999). *Documentation ARPEGE-Climat*. CNRM (Available from Centre National de Recherches Meteorologiques, Météo-France, Toulouse, France).

Eickhout, B., M. den Elzen and E. Kreileman (2001). *The atmospheric ocean system in IMAGE 2.2*. National Institute for Public Health and the Environment, Bilthoven, The Netherlands. *Tech. Rep. n°* 481508017.

Feddema, J., K. Oleson, G. Bonan, L. Mearns, W. Washington, G. Meehl and D. Nychka (2005a). A comparison of a GCM response to historical anthropogenic land cover change and model sensitivity to uncertainty in present-day land cover representations. *Climate Dyn, 25,* 581-609.

Feddema, J., K. Oleson, G. Bonan, L. Mearns, L. Buja, G. Meehl and W. Washington (2005b).The importance of land-cover change in simulating future climates. *Science, 310,* 1674-1678.

Fisher, G., H. van Velthuizen, F. Nechtergaele and S. Medow (2000). *CD-ROM: Global Agro-Ecological Zones*. Food and Agriculture Organization of United Nations, Rome, Italy; and International Institute for Applied Systems Analysis, Laxenburg, Austria.

Foley, J., I. Prentice, N. Ramankutty, S. Levis, D. Pollard, S. Sitch and A. Haxeltine (1996). An integrated biosphere model of land surface processes, terrestrial carbon balance, and vegetation dynamics. *Global Biogeochem. Cycles*, *10*, 603–628.

Frich, P.; L. Alexander, P. Della-Marta, B. Gleason, M. Haylock, A. Klein Tank (2002). Observed coherent changes in climate extremes during the second half of the twentieth century. *Clim. Res., 19*, 193-212.

Govindasamy, B., P. Duffy and K. Caldeira (2001). Land use changes and northern hemisphere cooling. *Geophys. Res. Lett.*, *28*, 291–294.

Henderson-Sellers, A., R. Dickinson, T. Dubridge, P. Kennedy, K. McGuffie and A. Pitman (1993). Tropical deforestation: modelling local- to regional-scale climate change. *J. Geophys. Res.*, *98*, 7289–7315.

Houghton, J., Y. Ding, D. Griggs, M. Noguer, P. van der Linden, X. Dai, K. Maskell and C. John/son (2001). *Climate Change 2001: The scientific basis*. Cambridge University Press, Cambridge, United Kingdom and New York.

Hulme, M., T. Wigley, E. Barrow, S. Raper, A. Centella, S. Smith and A. Chipanski (2000). *Using a climate scenario generator for vulnerability and adaptation assessments: MAGICC and SCENGEN version 2.4 workbook*. Climate Research Unit, Norwich, UK.

Joos, F., M. Bruno, R. Fink, U. Siegenthaler, T. Stocker, C. Le Quéré and J. Sarmiento (1996). An efficient and accurate representation of complex oceanic and biospheric models of anthropogenic carbon uptake. *Tellus*, *48B*, 397–417.

Lean, J. and P. Rowntree (1997). Understanding the sensitivity of a GCM simulation of Amazonian deforestation to the specification of vegetation and soil characteristics. *J. Climate.*, *10*, 1216–1235.

Leemans R. and G.J. van den Born (1994). Determining the potential global distribution of natural vegetation, crops and agricultural productivity. *Wat. Air Soil Pollut.*, *76*, 133–162.

Louis, J. F., M. Tiedke and J. F. Geleyn (1982). A short history of the operational PBL-parameterization at ECMWF. *ECMWF Workshop Planetary Boundary Layer Parameterization.* ECMWF, Reading, UK. 59–80.

Madec, G., P. Delecluse, M. Imbard and C. Lévy (1997). *OPA version 8.0 Ocean General Circulation Model Reference Manual*. LODYC (Available from Laboratoire d'Océanographie Dynamique et de Climatologie, IPSL, Paris 75252, France).

Mahfouf, J.-F., A. Manzi, J. Noilhan, H. Giordani and M. Déqué (1995). The land surface scheme ISBA within the Météo-France climate model ARPEGE Part I: Implementation and preliminary results. *J. Climate.*, *8*, 2039–2057.

Masson, V., J. L. Champeaux, F. Chauvin, C. Meriguet and R. Lacaze (2003). A global database of land surface parameters at 1km resolution in meteorological and climate models. *J. Climate.*, *16*, 1261–1282.

Matthews, H., A. Weaver, K. Meissner, N. Gillett and M. Eby (2004). Natural and anthropogenic climate change: incorporating historical land cover change, vegetation dynamics and the global carbon cycle. *Climate Dyn.*, *22*, 461–479. DOI: 10.1007/s00382-004-0392-2 .

Morcrette, J. J. (1990). Impact of changes to the radiation transfer parameterizations plus cloud optical properties in the ECMWF model. *Mon. Weather. Rev.*, *118*, 847–873.

Nakicenovic, E., J. Alcamo, J. Davis, B. de Vries, J. Fenhann, S. Gaffin, K. Gregory, A. Grübler, Y. Jung, T. Kram, E. La Rovere, L. Michaelis, S. Mori, T. Morita, W. Pepper, H. Pitcher, L. Price, K. Riahi, A. Roehrl, H. Rogner, A. Sankovski, M. Schlesinger, P. Shukla, S. Smith, R. Swart, S. van Rooijen, N. Victor and Z. Dadi (2001). *IPCC Special report on emissions scenarios*. Cambridge University Press, Cambridge, United Kingdom and New York.

Notaro, M., Z. Liu, R. Gallimore, S. Vavrus and J. Kutzbach (2005). Simulated and observed preindustrial to modern vegetation and climate changes. *J. Climate.*, *18*, 3650–3671.

Oki, T. and Y. Sud (1998). Design of Total Runoff Integrating Pathways (TRIP): a global river channel network. *Earth Interactions, 2,* paper 1.

Parmesan, C., T. Root and M. Willig (2000). Impacts of extreme weather and climate on terrestrial biota. *Bull. Am. Meteorol. Soc., 81*, 443-450.

Pitman, A. and M. Zhao (2000). The relative impact of observed change in land cover and carbon dioxide as simulated by a climate model. *Geophys. Res. Lett.*, *27*, 1267–1270.

Prentice, I., W. Cramer, S. Harrison, R. Leemans, R. Monserud and A. Solomon (1992). A global biome model based on plant physiology and dominance, soil properties and climate. *J. Biogeography*, *19*, 117–134.

Ricard, J. L. and J. F. Royer (1993). A statistical cloud scheme for use in an AGCM. *Ann. Geophysicae.*, *11*, 1095–1115.

Salas-Mélia, D. (2002). A global coupled sea ice-ocean model. *Ocean Mod.*, *4*, 137–172.

Salas-Mélia, D., F. Chauvin, M. Déqué, H. Douville, J. Guérémy, P. Marquet, S. Planton, J. Royer and S. Tyteca (2006). Description and validation of the CNRM-CM3 global coupled model. CNRM, *Note de Centre n°103.*

Schlesinger, M.E., S. Malyshev, E.V. Rozanov et al. (2000). Geographical distributions of temperature change for scenarios of greenhouse gas and sulfur dioxide emissions. *Technological Forecasting and Social Change, 65,* 167–193.

Seguin, B. (2005). Impacts sur l'agriculture. *Changements climatiques: quels impacts en france?* 100–107.

Sitch, S., I. Prentice, B. Smith, W. Cramer, J. Kaplan, W. Lucht, S. M., K. Thonike and S. Venevsky (2003). LPJ- A coupled model for vegetation dynamics and the terrestrial carbon cycle. *Global Change Biology*, *9*, 161–185.

Sud, Y., G. Walker, J. Kim, G. Liston, P. Sellers and W. Lau (1996). Biogeophysical consequences of a tropical deforestation scenario: a GCM simulation study. *J. Climate.*, *9*, 3225–3247.Taylor, C., E. Lambin, N. Stephenne, R. Harding and R. Essery (2002). The influence of land use change on climate in the Sahel. *J. Climate.*, *15*, 3615–3629.

Taylor, C., E. Lambin, N. Stephenne, R. Harding and R. Essery (2002). The influence of land use change on climate in the Sahel. *J. Climate.*, *15*, 3615–3629.

Terray, L., S. Valcke and A. Piacentini (1998). *OASIS 2.2 User's guide and reference manual*. CERFACS.

Van Minnen, J. G., R. Leemans and F. Ihle (2000). Defining the importance of including transient ecosystem responses to simulate C-cycle dynamics in a global change model. *Global Change Biology, 6,* 595–612 .

Voldoire, A. (2006). Quantifying the impact of future land-use changes against increases in GHG concentrations. *Geophys. Res. Lett.*, *33(4)*. DOI: 1029/2005GL024354

Voldoire, A. and J. Royer (2004). Tropical deforestation and climate variability. *Climate Dyn.*, *22*, 857-874. DOI:10.1007/s00382-004-0423-z.

Wang, G., E. Eltahir, J. Foley, D. Pollard and S. Levis (2004). Decadal variability of rainfall in the Sahel: results from the coupled GENESIS-IBIS atmosphere-biosphere model. *Climate Dyn.*, *22*, 625–637. DOI: 10.1007/s00382-004-0411-3.

Zhao, M. and A. Pitman (2002). The regional scale impact of land cover change simulated with a climate model. *Int. J. of Climatol.*, *22*, 271–290.

Tables

Experiment	Models used
A2-IM-CM3	New coupled system IMAGE2.2/CNRM-CM3
A2-CM3	CNRM-CM3 alone, prescribed forcings from IPCC
A2-IM	IMAGE2.2 alone, with its own climate module
A2-IM-forced	IMAGE2.2 forced with climate change given by A2-CM3

Table 1: Experiments performed

		Averaged value over the period 1961-1999	Averaged value over the period 1970-2099	Difference
Quantile 90% of daily maximum temperature	A2-CM3	34.2	39.3	**+5.1**
	A2-IM-CM3	32.0	37.6	**+5.6**
Quantile 10% of daily maximum temperature	A2-CM3	25.4	28.8	**+3.4**
	A2-IM-CM3	25.2	29.0	**+3.8**
Quantile 10% of daily minimum temperature	A2-CM3	17.7	22.7	**+5.0**
	A2-IM-CM3	19.4	24.0	**+4.6**
Quantile 90% of daily minimum temperature	A2-CM3	23.3	28.0	**+4.7**
	A2-IM-CM3	24.0	28.6	**+4.6**
Nb of days with precip greater than 10mm.d^{-1}	A2-CM3	36.0	38.9	**+2.8**
	A2-IM-CM3	32.5	33.2	+0.8
Maximum rainfall over 5 days (mm)	A2-CM3	127	159	**+32**
	A2-IM-CM3	125	152	**+27**
Maximum nb of consecutive dry days	A2-CM3	41.5	39.4	-2.1
	A2-IM-CM3	36.3	44.0	**+7.7**

Table2 : Change in extreme indices averaged over the Amazonian region **[**10S-5N, 30W-80W] for the simulation A2-IM-CM3 and A2-CM3. These indices were defined in the Stardex project (see http://www.cru.uea.ac.uk/cru/projects/stardex) and are described in Frich et al. (2002). Differences are bolded when they are significant at the 99% level according to a Student's t-test.

Figure captions

Figure 1: Change in Leaf Area Index (LAI) in 2090-2099 compared to 1970-1979, for different latitude bands, according to the IMAGE2.2 land cover simulations for the A2 scenario. In the "Natural vegetation only" case, the map considered is the natural vegetation map simulated by IMAGE, in the absence of any land-use. In the other case, the anomaly is taken for the land cover map including the land-use distribution.

Figure 2: IMAGE2.2 model flow diagram (http://www.mnp.nl/image/).

Figure 3: Coupling of the CNRM-CM3 GCM and the IMAGE2.2 model. The two models are coupled asynchronously every 5 years.

Figure 4: Concentration scenario in CO_2 (top), CH_4 (middle) and N_2O (bottom) for the simulations listed in table 1.

Figure 5: Global mean annual near surface temperature for the IPCC CNRM-CM3 simulation (A2-CM3) and the simulation with the new coupled system including IMAGE2.2 (A2-IM-CM3).

Figure 6: a) Sea-ice cover in the northern hemisphere for simulations A2-CM3 and A2-IM-CM3. b) the corresponding 10 year trends calculated following a linear regression on the 10 year window centered on the year considered, the dotted lines indicate the minimum and maximum trend obtained with the same method over a 500 year control simulation with the CNRM-CM3 model using constant pre-industrial forcings, the dashed lines indicates the 5% and 95% percentiles from the same run and gives an indication of the significance of the results.

Figure 7: Initial year beginning the first period for which A2-IM-CM3 is warmer than A2-CM3 over ten years in a row on annual mean values.

Figure 8: Evolution of a) the vegetation fraction, b) the vegetation albedo, c) the Leaf Area Index (LAI) and d) the rooting depth averaged over 3 zonal regions 60N-90N (top), 30N-60N (middle), 30S-30N (bottom) in the A2-IM-CM3 simulation (red curve). Orange triangles indicate the same diagnostics for A2-CM3 in which land-cover is kept constant.

Figure 9: Annual mean leaf area index in (1) A2-IM-CM3 in 1970, (2) A2-CM3, (3) and the difference A2-IM-CM3 minus A2-CM3.

Figure 10: Change in annual mean near surface temperature between the period 2070-2099 and the period 1960-1989 normalized by global mean change, for A2-IM-CM3 (a) and A2-CM3 (b) and the difference between these anomalies (c) with contours indicating significant differences following a Student t-test with 95% and 99% significance level.

Figure 11: Change in annual mean precipitation ($mm.day^{-1}$) between the period 2070-2099 and the period 1960-1989 for A2-IM-CM3 (a) and A2-CM3 (b), and the difference of the anomalies between the two experiments (c). Contours indicate the significance following a student t-test with 95% and 99% of significance level.

Figure 12: Land cover obtained in the A2-IM-CM3 simulation for 1970 (top), 2100 (middle), and for 2100 but only for grid points where there have been a change (bottom).

Figure 13: Change in annual mean daily temperature range over the Amazonian region [10S-5N, 30W-80W] between the period 2070-2099 and the period 1960-1989 for the simulations A2-CM3, A2-IM-CM3, A1B-CM3 and B1-CM3. A1B-CM3 and B1-CM3 are IPCC4 simulations run with CNRM-CM3 for scenario A1B and B1.

Figure 14: Area of crops over the Amazonian region [10S-5N, 30W-80W] (top) and area of boreal forests north of 70°N (bottom) for A2-IM-CM3 and an ensemble of IMAGE simulations forced with different climate change projections. The different simulations of the ensemble are named following the same rule. A1B-CM3_B1 means that IMAGE has been run for an A1B narrative with a climate change taken from a simulation with CNRM-CM3 for scenario B1. The term fix refers to simulations in which no climate change is taken into account.

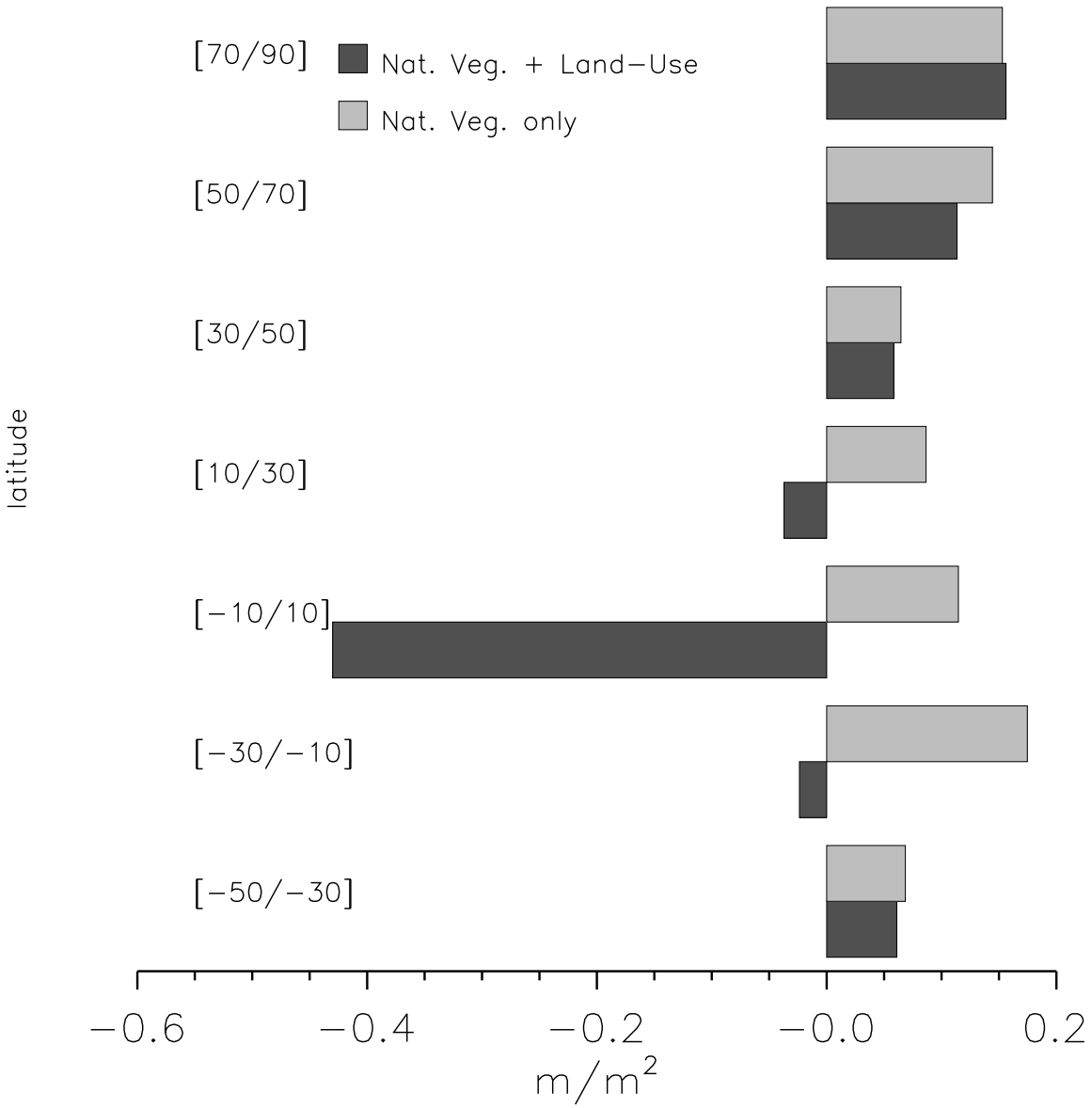
[70/90]
Nat. Veg. + Land−Use
Nat. Veg. only
[50/70]
[30/50]
[10/30]
[−10/10]
[−30/−10]
[−50/−30]
latitude
−0.6
−0.4
−0.2
−0.0
0.2
m/m²

Figure 1:

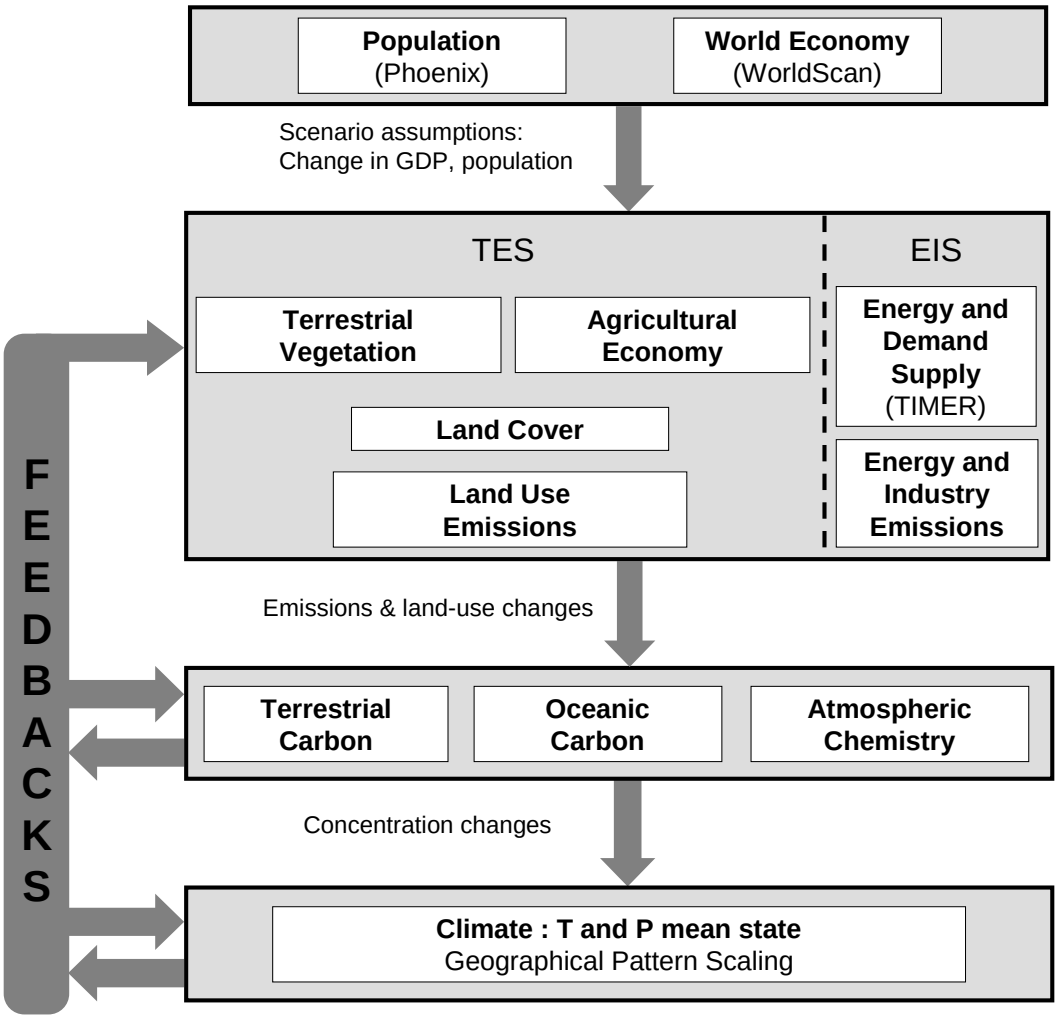
Population
(Phoenix)
World Economy
(WorldScan)
Scenario assumptions:
Change in GDP, population
TES
EIS
Terrestrial Vegetation
Agricultural Economy
Energy and Demand Supply
(TIMER)
Land Cover
Land Use Emissions
Energy and Industry Emissions
Emissions & land-use changes
Terrestrial Carbon
Oceanic Carbon
Atmospheric Chemistry
Concentration changes
Climate : T and P mean state
Geographical Pattern Scaling
FEEDBACKS

Figure 2:

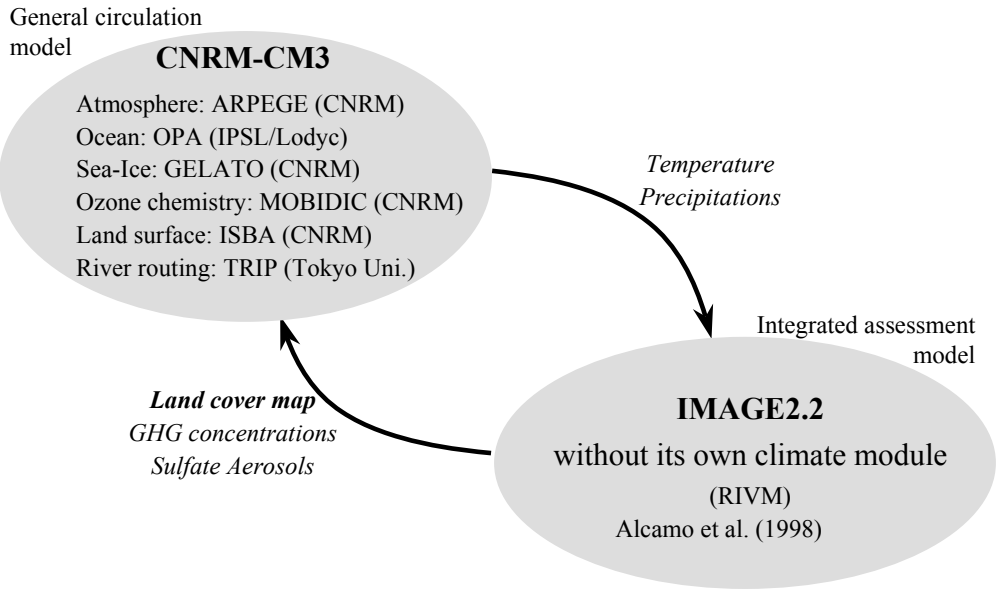
General circulation model
CNRM-CM3
Atmosphere: ARPEGE (CNRM)
Ocean: OPA (IPSL/Lodyc)
Sea-Ice: GELATO (CNRM)
Ozone chemistry: MOBIDIC (CNRM)
Land surface: ISBA (CNRM)
River routing: TRIP (Tokyo Uni.)
Temperature
Precipitations
Integrated assessment model
IMAGE2.2
without its own climate module
(RIVM)
Alcamo et al. (1998)
Land cover map
GHG concentrations
Sulfate Aerosols

Figure 3:

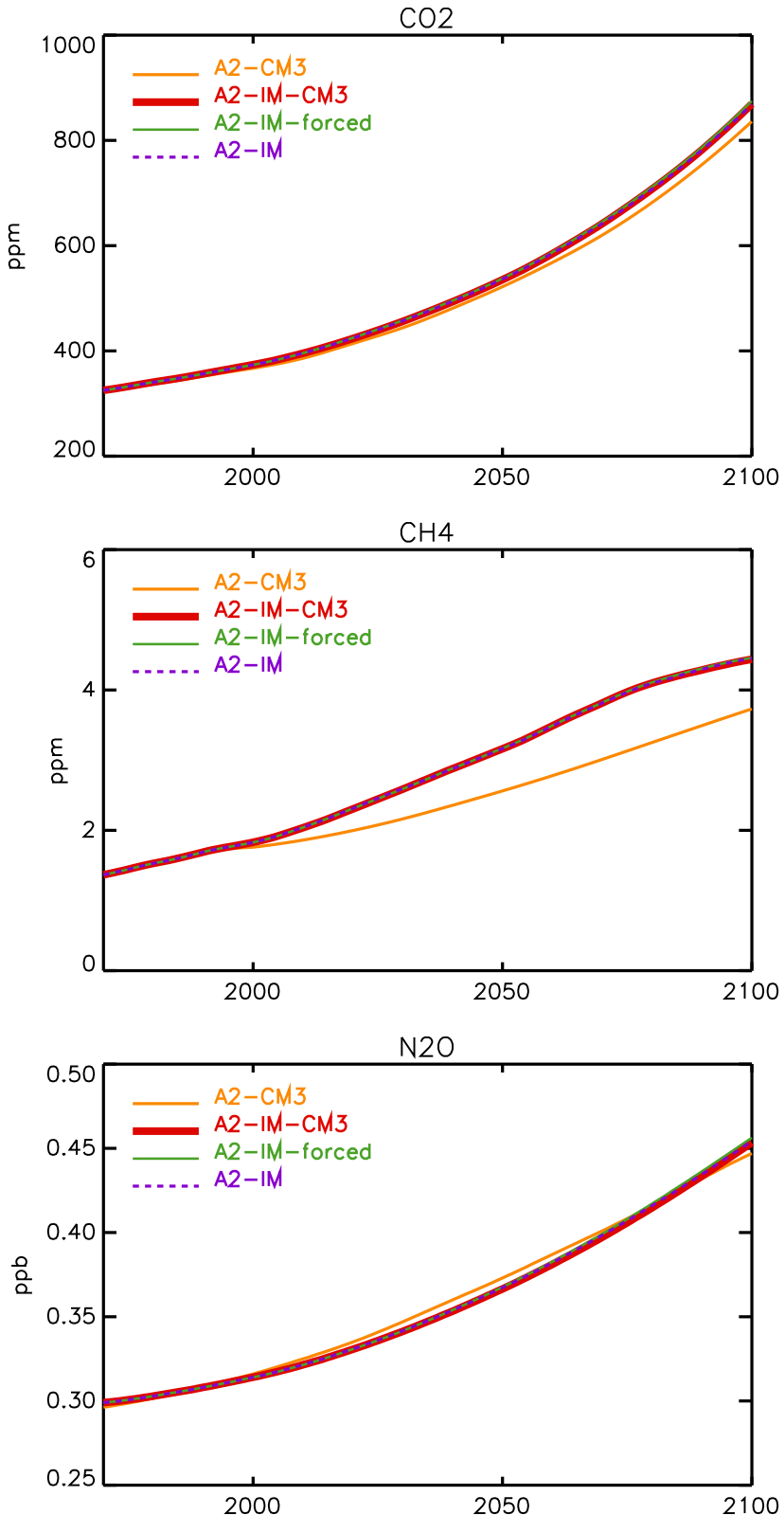
CO2
1000
800
600
400
200
ppm
2000
2050
2100
A2−CM3
A2−IM−CM3
A2−IM−forced
A2−IM
CH4
6
4
2
0
ppm
2000
2050
2100
A2−CM3
A2−IM−CM3
A2−IM−forced
A2−IM
N2O
0.50
0.45
0.40
0.35
0.30
0.25
ppb
2000
2050
2100
A2−CM3
A2−IM−CM3
A2−IM−forced
A2−IM

Figure 4:

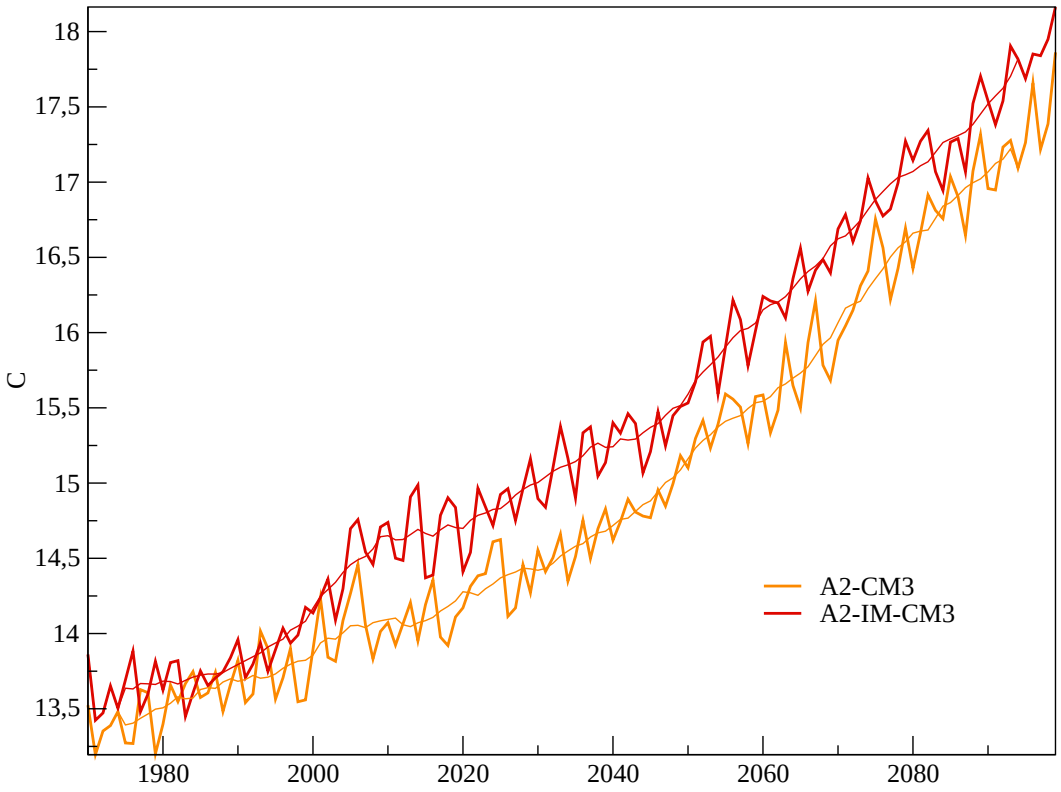
18
17,5
17
16,5
16
15,5
15
14,5
14
13,5
C
1980
2000
2020
2040
2060
2080
A2-CM3
A2-IM-CM3

Figure 5:

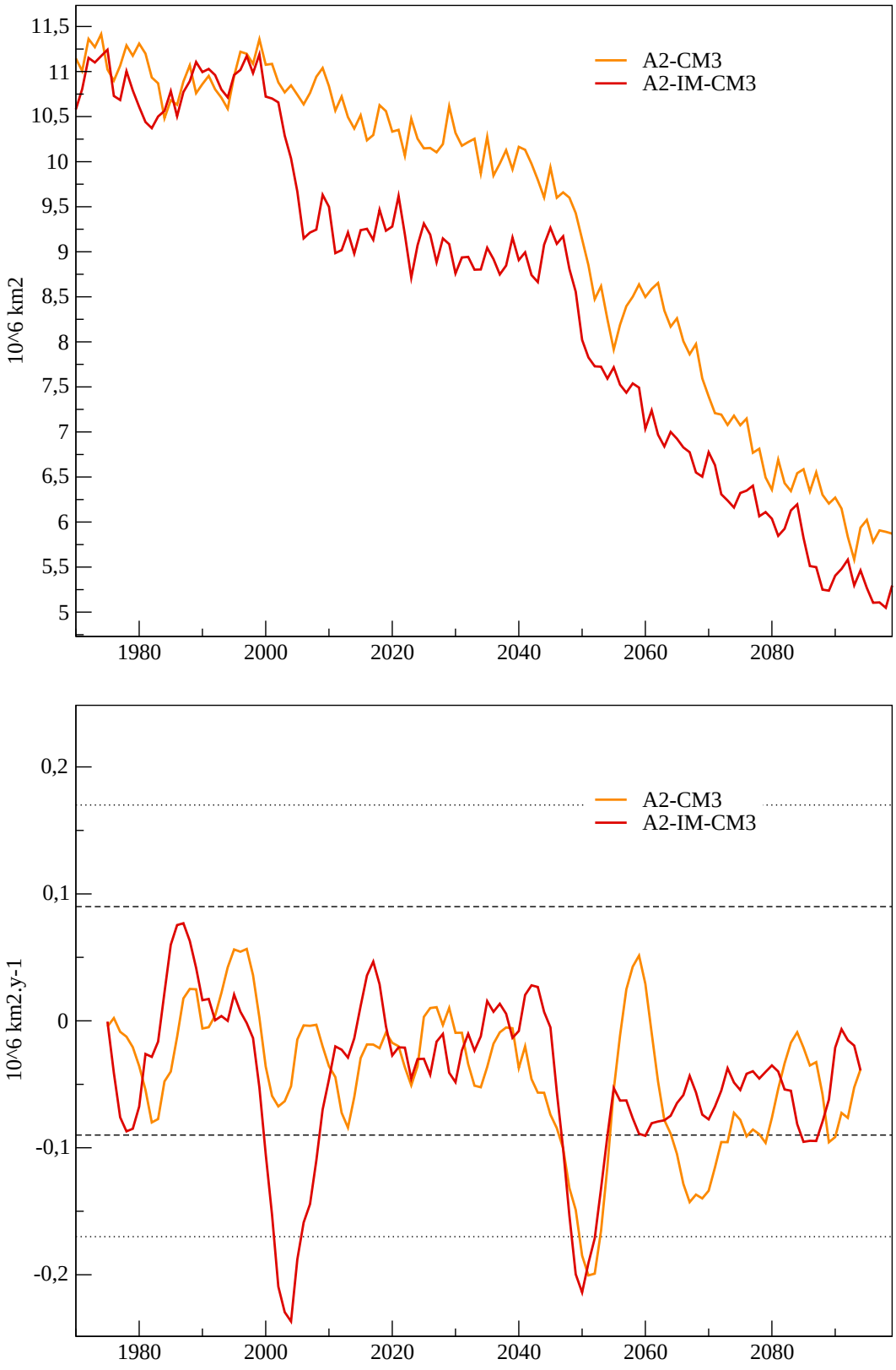
11,5
11
10,5
10
9,5
9
8,5
8
7,5
7
6,5
6
5,5
5
10^6 km2
A2-CM3
A2-IM-CM3
1980
2000
2020
2040
2060
2080
0,2
0,1
0
-0,1
-0,2
10^6 km2.y-1
A2-CM3
A2-IM-CM3
1980
2000
2020
2040
2060
2080

Figure 6:

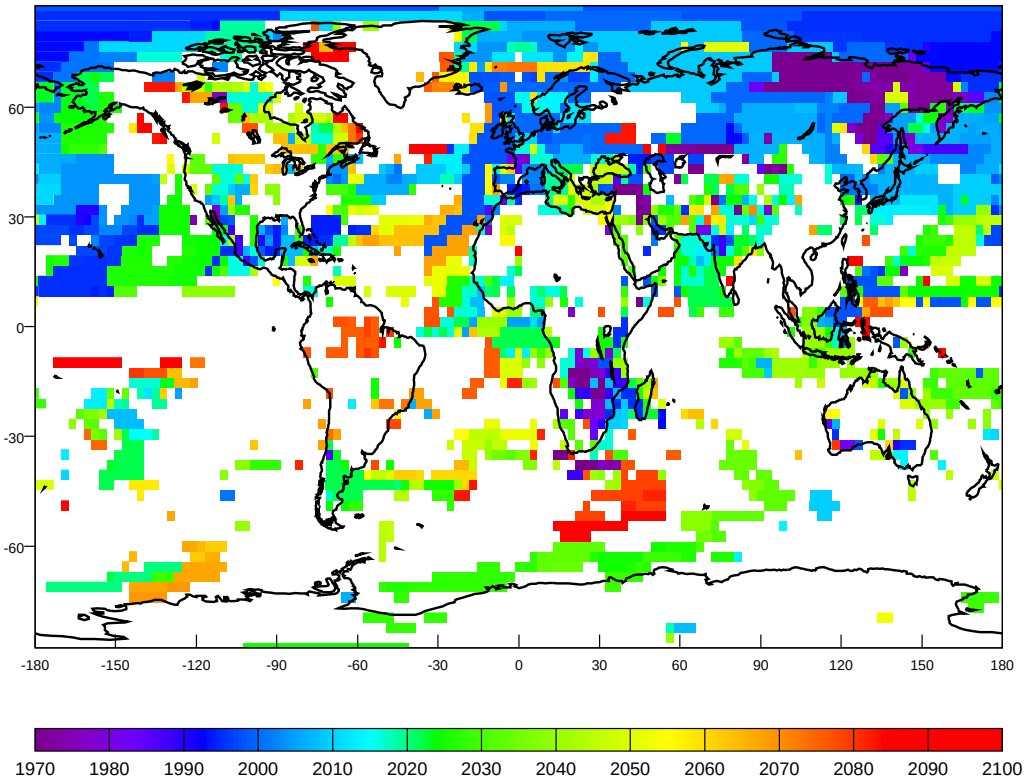
60
30
0
-30
-60
-180
-150
-120
-90
-60
-30
0
30
60
90
120
150
180
1970
1980
1990
2000
2010
2020
2030
2040
2050
2060
2070
2080
2090
2100

Figure 7:

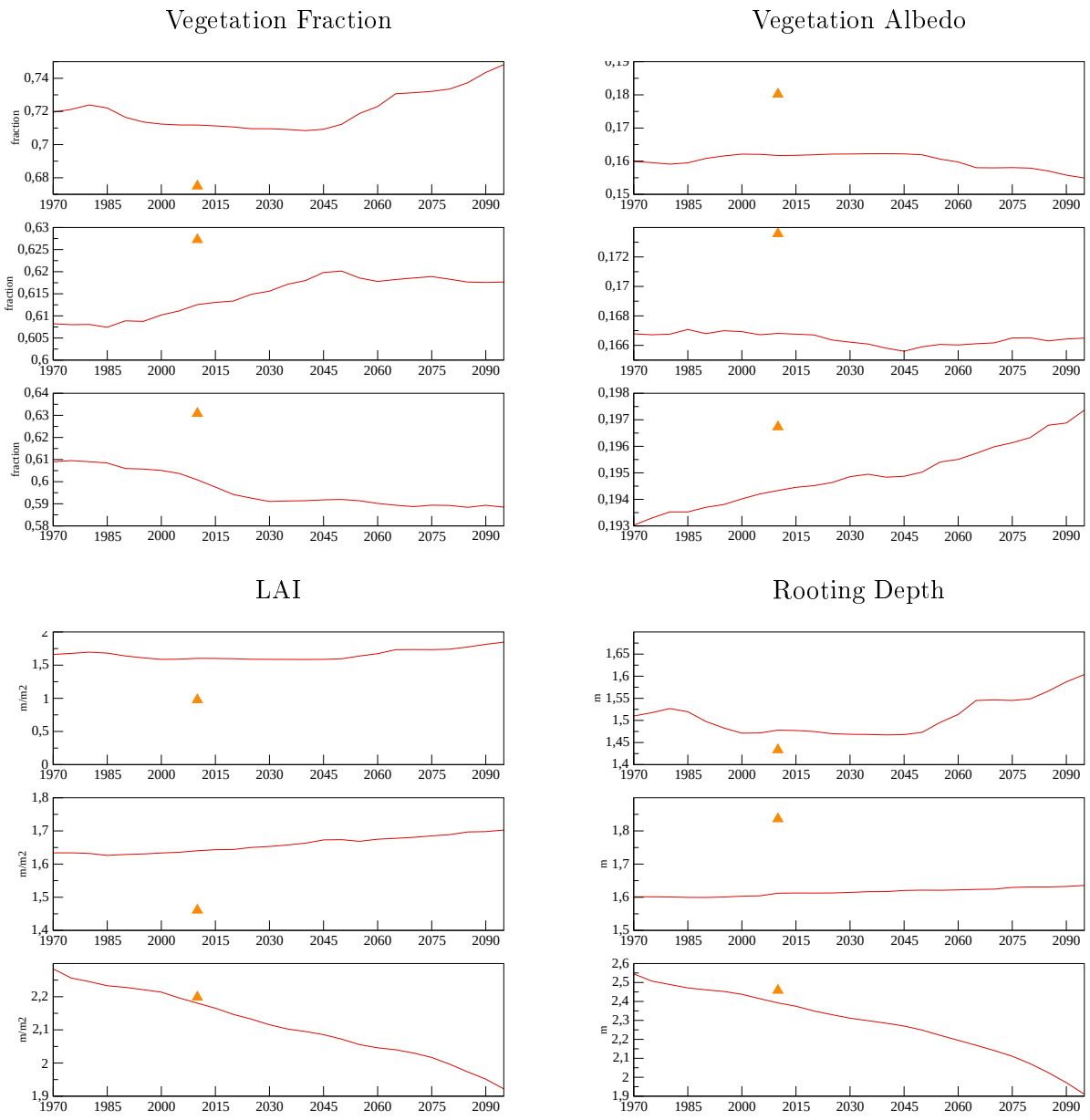
Vegetation Fraction
Vegetation Albedo
LAI
Rooting Depth
fraction
m/m2
m

Figure 8:

(a) A2-IM-CM3 (1970)

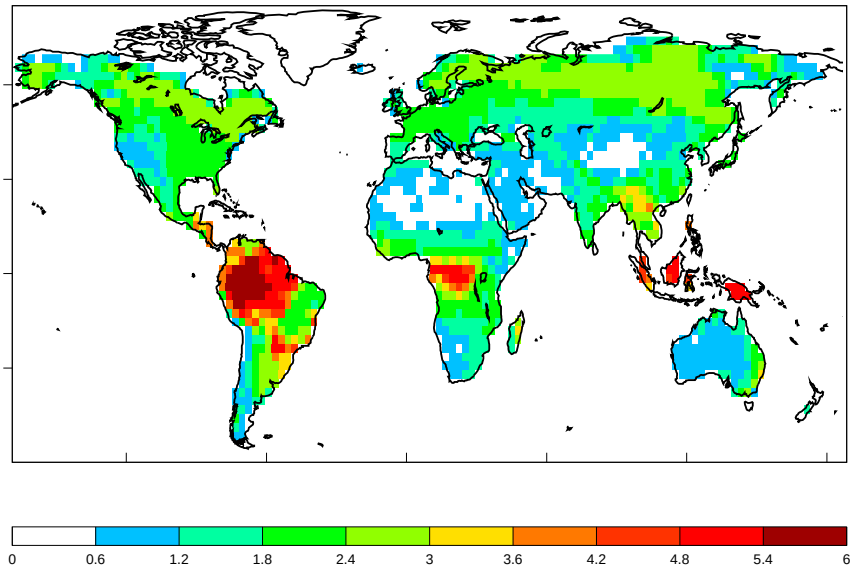

(b) A2-CM3

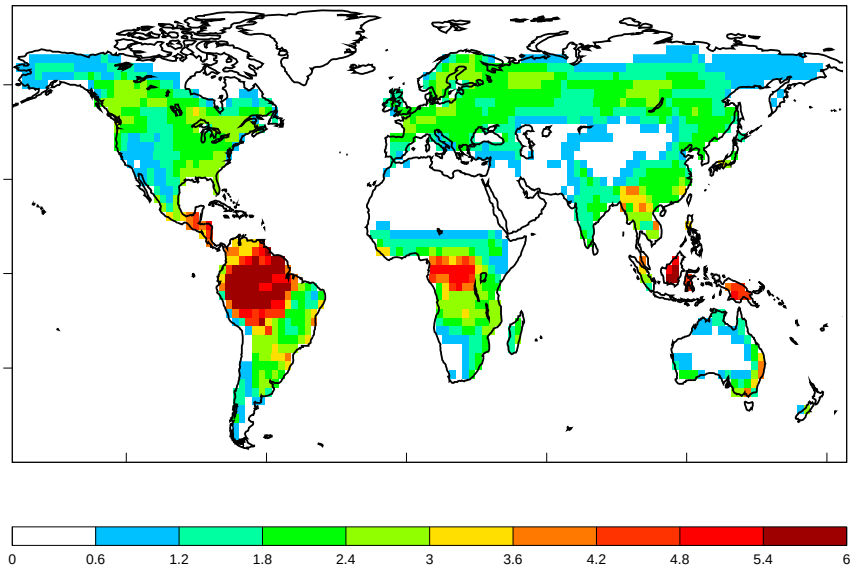

(c) = (a) - (b)

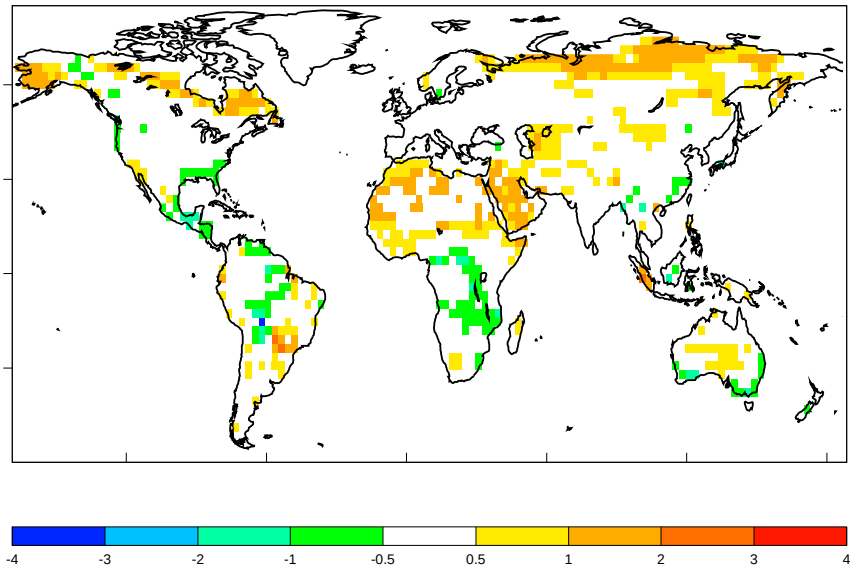

Figure 9:

(a) A2-IM-CM3

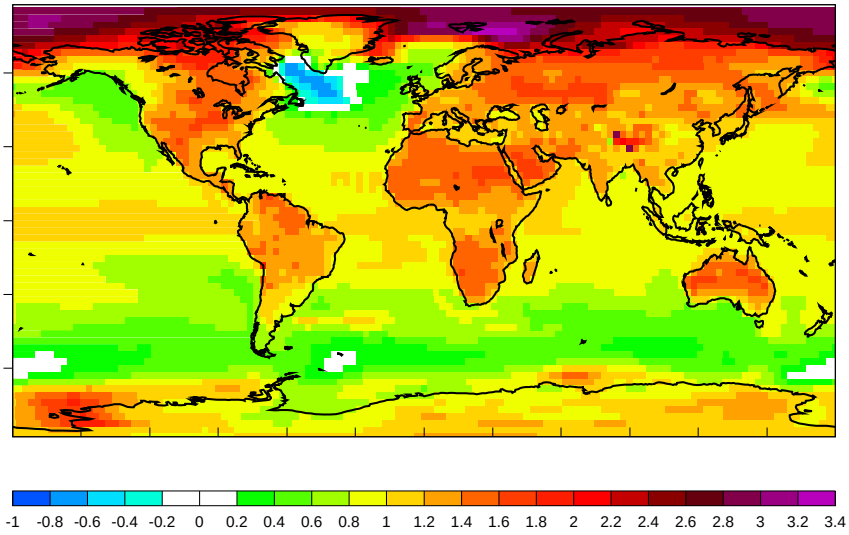

(b) A2-CM3

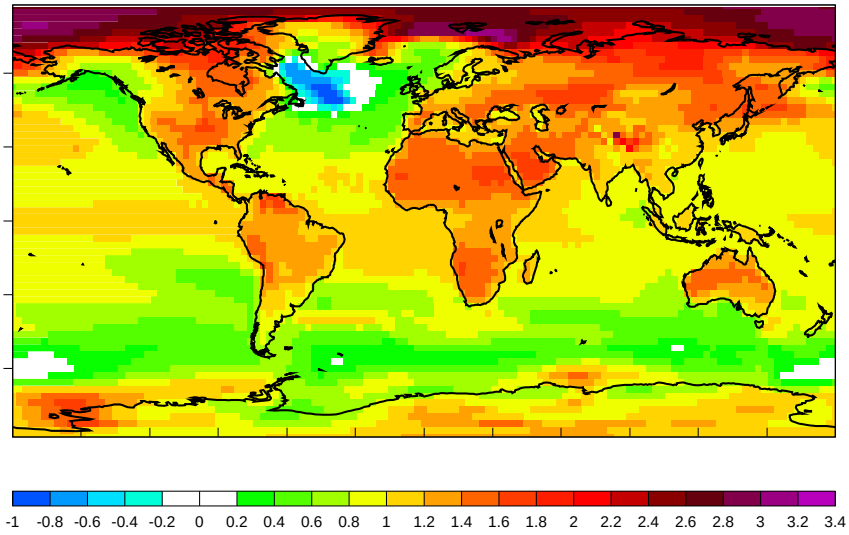

(c) = (a) - (b)

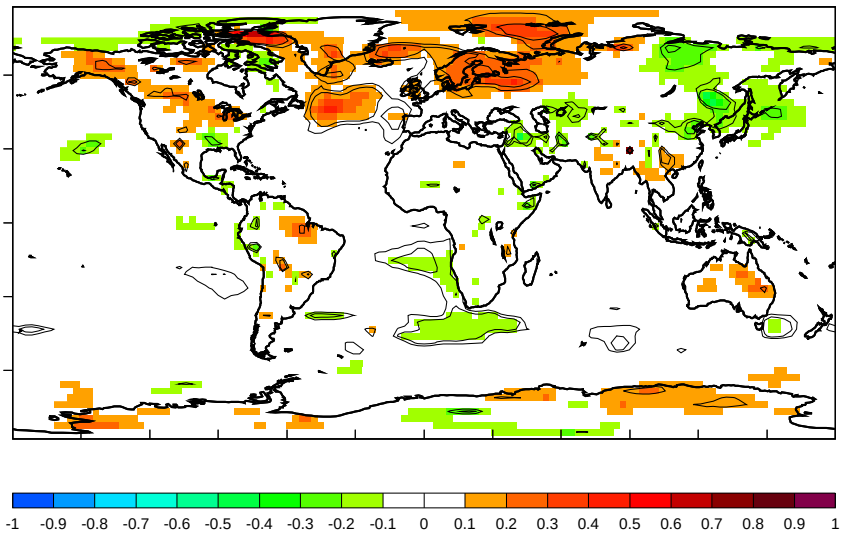

Figure 10:

(a) A2-IM-CM3

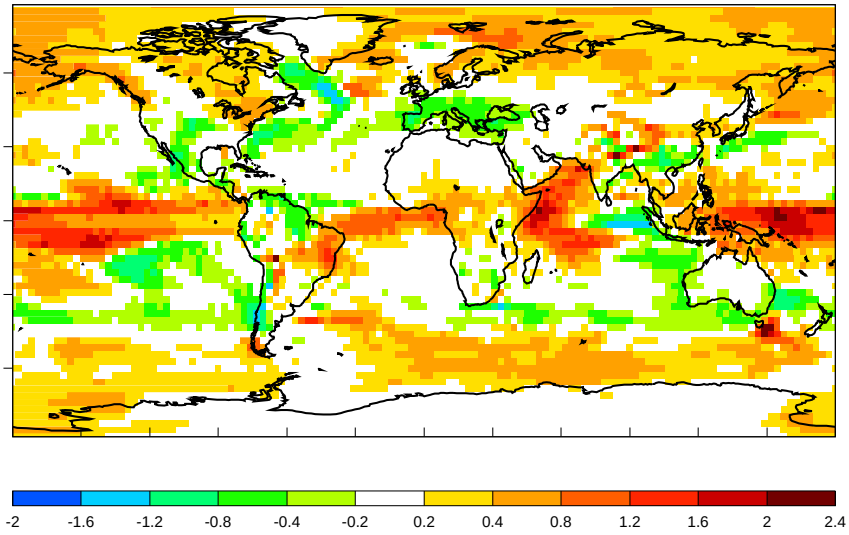

(b) A2-CM3

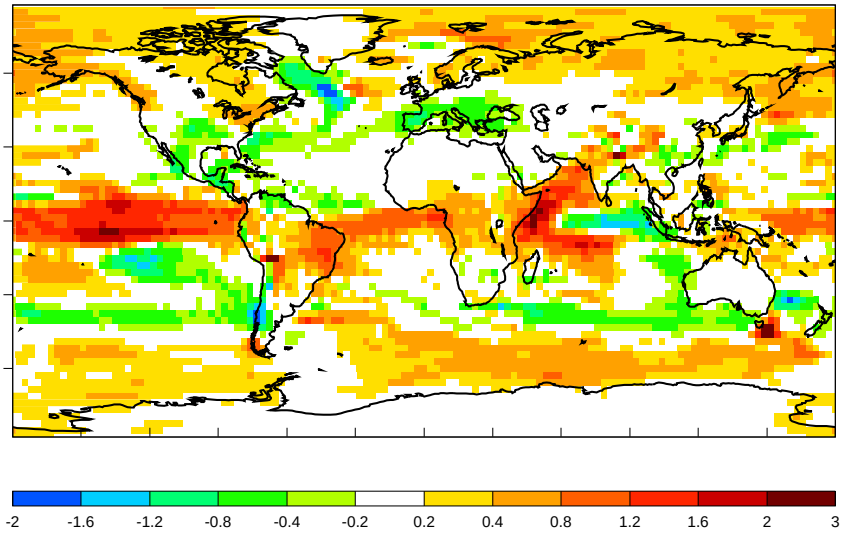

(c) = (a) - (b)

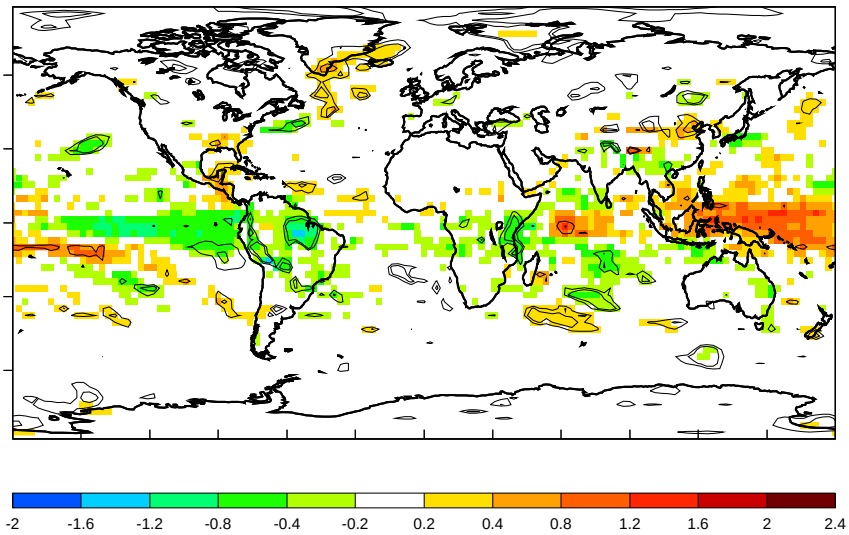

Figure 11:

1970

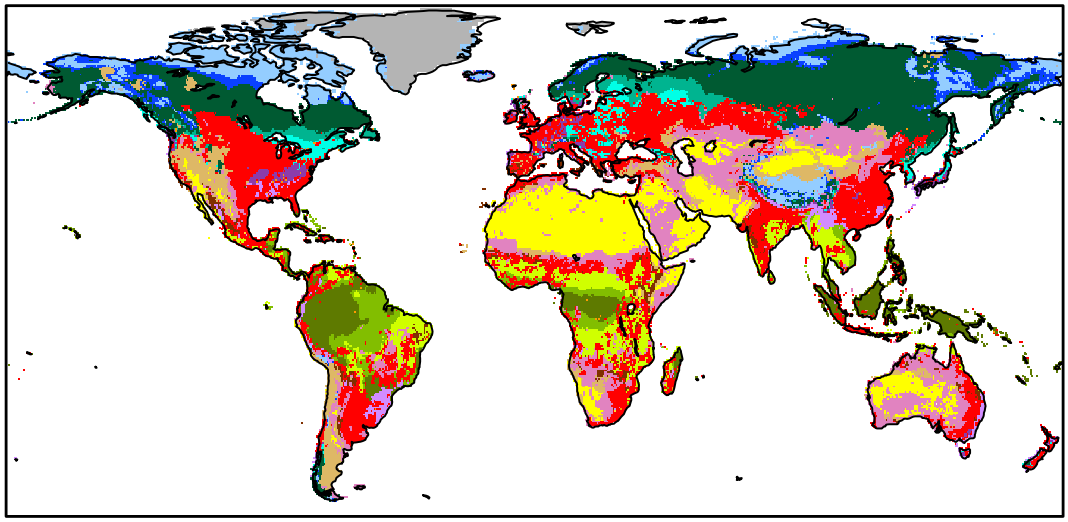

2100

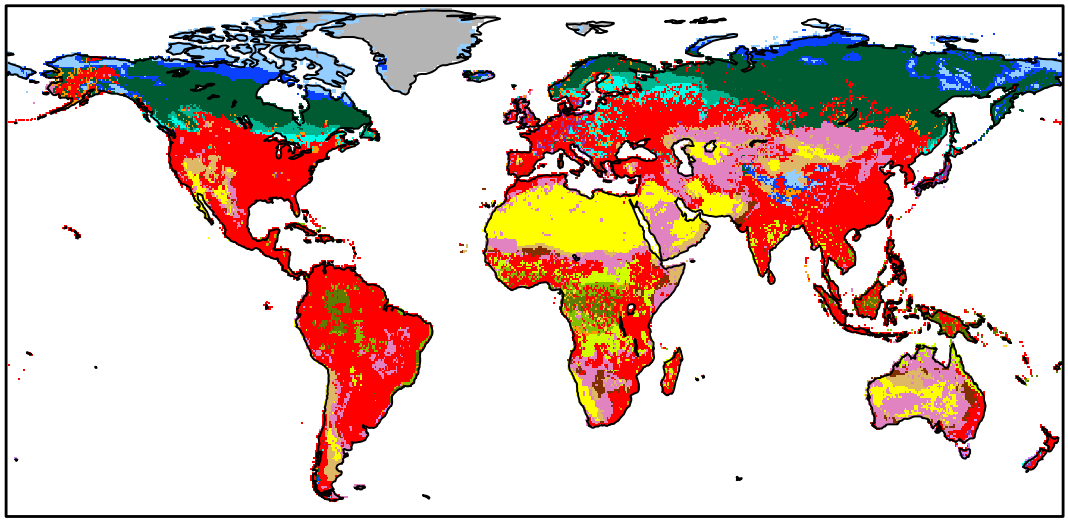

where 2100 is different from 1970

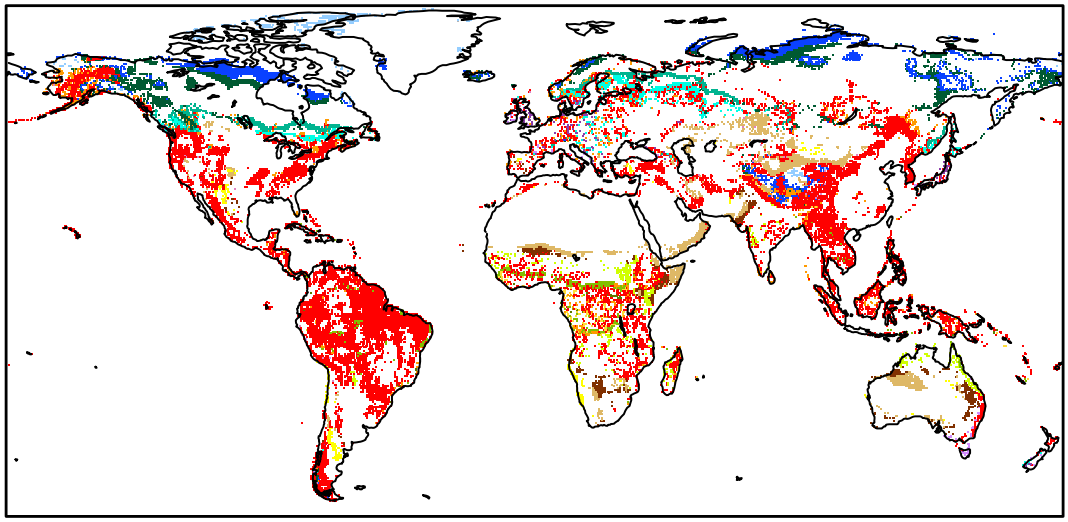

Figure 12:

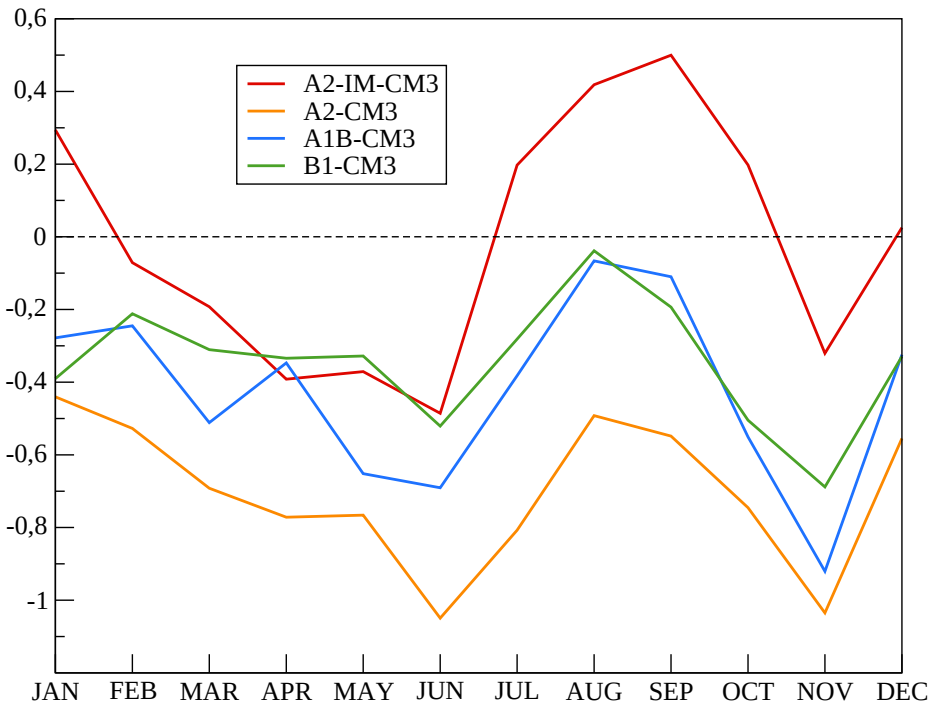
0,6
0,4
0,2
0
-0,2
-0,4
-0,6
-0,8
-1
A2-IM-CM3
A2-CM3
A1B-CM3
B1-CM3
JAN
FEB
MAR
APR
MAY
JUN
JUL
AUG
SEP
OCT
NOV
DEC

Figure 13:

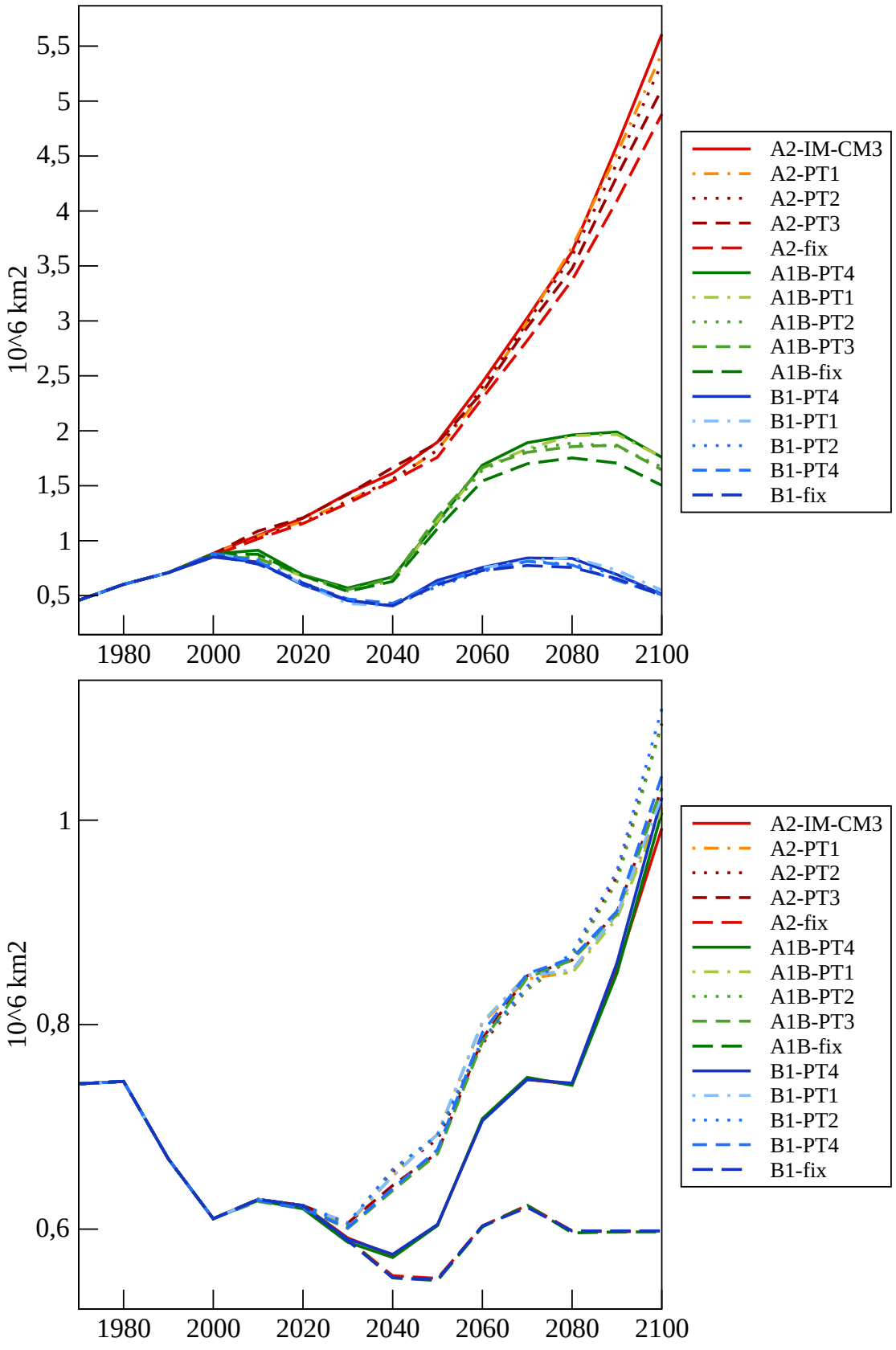
10^6 km2
5,5
5
4,5
4
3,5
3
2,5
2
1,5
1
0,5
1980
2000
2020
2040
2060
2080
2100
A2-IM-CM3
A2-PT1
A2-PT2
A2-PT3
A2-fix
A1B-PT4
A1B-PT1
A1B-PT2
A1B-PT3
A1B-fix
B1-PT4
B1-PT1
B1-PT2
B1-PT4
B1-fix
10^6 km2
1
0,8
0,6
1980
2000
2020
2040
2060
2080
2100
A2-IM-CM3
A2-PT1
A2-PT2
A2-PT3
A2-fix
A1B-PT4
A1B-PT1
A1B-PT2
A1B-PT3
A1B-fix
B1-PT4
B1-PT1
B1-PT2
B1-PT4
B1-fix

Figure 14: